Journal of Engineering and Applied Sciences 13 (Special Issue 10): 8188-8195, 2018
ISSN: 1816-949X

Study of Fluidizing System Behavior Using Nanoparticles

Jamal M. Ali and Sarah T. Hussian
Department of Chemical Engineering, University of Technology, Baghdad, Iraq

Abstract: The fluidization characteristics or hydrodynamic behavior of nanoparticles (mixtures of 30 and 100 nm diameter particles) and microparticles (d_p = 75 μm) of Aluminum Oxide (Al_2O_3) were studied in a fluidized bed of a gas-solid system. Experiments were performed in two cylindrical columns the first column with a diameter of D = 4.3 cm and the second with a diameter of D = 7.1 cm by varying different system parameters (viz., static bed height, particle size and superficial gas velocity) using air as the fluidizing gas. Vibration technique was used for nanoparticle fluidization to avoid nanoparticle agglomeration. A simple analytical model is used to predict the agglomerate sizes for Al_2O_3 nanoparticles. The average agglomerate size was calculated using Stoke's law and the minimum fluidization velocity was calculated using the Ergun equation. The minimum fluidization velocity was 0.0183-0.046 m/sec without vibration and 0.0163-0.033 m/sec with vibration in the column with D = 4.3 cm for different static bed heights (5, 10 and 15 cm). In the column with D = 7.1 cm, the minimum fluidization velocity was 0.025-0.05 m/sec without vibration and 0.022-0.037 m/sec with vibration for different static bed heights (5, 7 and 10 cm). In addition, the fluidization behavior for Al_2O_3 microparticles was studied and the minimum fluidization velocity was calculated using the Ergun equation. In this case, the minimum fluidization velocity was 0.034-0.050 m/sec for the column with D = 4.3 cm and 0.063-0.070 m/sec for the column with D = 7.1 cm. Fluidization characteristics such as the bed expansion ratio, bed fluctuation ratio, bed pressure drop and the Fluidization Index (FI) of nanoparticles are described and discussed. The calculated values for different fluidization characteristics are compared with the experimentally observed values. A comparison of the results shows consistency between the experimental and calculated values for nanoparticles.

Key words: Fluidization, nanoparticle, agglomerate sizes, vibration, minimum fluidization velocity, microparticles

INTRODUCTION

Gas fluidization of nanoparticles employed immense in various manufacturing on account of its unusual capability of continuous powder treatment, good admix, great gas solid osculate area and notably hard to reach rates of heat and mass transfer (Zhu *et al*., 2005). Nano materials have attracted attention because of their unique physical, chemical and mechanical properties that differ from bulk solids and molecules. The notably large surface area of nanomaterial is one of the reasons for their unusual properties.

The agglomeration of nanoparticles is a ubiquitous phenomenon in the gas-phase processing of nanoparticles because of attractive forces such as van der Waals, electrostatic and capillary forces and hydrogen bonds which form between the surfaces of wet and dry nanoparticles. The fluidization of nanoparticles becomes much more difficult upon agglomeration. The Vibratory Fluidized Bed (VFB) has been demonstrated to be an effective means to overcome the cohesive forces among nanoparticles through an external vibration force (Zhu *et al*., 2004). The Ergun and Richardson Zaki equations are the principle models used to calculate the size of agglomerates in VFB. The fluidization of Al_2O_3 nanoparticles and microparticles has been extensively studied. Nanoparticle agglomerates can be smoothly fluidized if the gas velocity is increased far above (approximately several orders of magnitude) the minimum fluidization velocity of the primary nanoparticles. The important theme of this research is to empirical calculated the fluidization characteristics of diverse nanoparticles such as the minimum fluidization velocity, agglomerate size, bed expansion, pressure drop and fluidization index. In this research, we investigated the effect of vibration on the fluidization quality and compared nanoparticle and micro particle fluidization behaviors.

MATERIALS AND METHODS

A schematic of the vibro fluidization system is shown in Fig. 1. The system comprises vibration device and two fluidized beds of nanoparticle agglomerates. The fluidized beds are vertical transparent columns, each with a distributor at the bottom. The two fluidizing columns are cylindrical transparent Perspex tubes to minimize

Corresponding Author: Jamal M. Ali, Department of Chemical Engineering, University of Technology, Baghdad, Iraq

Table 1: Physical properties of the solids

Powder	Color	Shape	Primary particles	True density	Assay size (%)	Molecular weight (kg/m^2)
Al_2O_3	White	Crystalization	30 and 100 nm	3960	99	101.96
Al_2O_3	White	Crystalization	≤75 μm	3960	99	101.96

Fig. 1: The experimental setup

electrostatic charge and one end is fixed to a Perspex flange. The diameter and height of the first column are 4.3 and a 100 cm, respectively; those of the second column are 7.1 and 100 cm, respectively. Each distributor at the bottom of the fluidized beds consists of a ceramic plate approximately 5 mm thick with a pore size from 2.4 putted at the gas outlet to filter out any efflux of nanoparticle agglomerates. The pressure drop across the fluidized bed was measured using a digital manometer which was connected to a pressure tap that positioned immediately above the gas distributor. The gas flow rate was measured using a series of rotameters. An electric motor was connected to the power source on the outer surface of the column by metal girdle to induce vibrations with a frequency f of approximately 50 Hz.

The physical properties of the Al_2O_3 nanoparticles and microparticles are listed in Table 1. The Al_2O_3 nanoparticlesare clearly at the extreme end of Geldard's group C powder classification.

RESULTS AND DISCUSSION

The reported results are the average value of several readings obtained with satisfactory repeatability. The results are presented in two sections: the fluidization behavior of nanoparticles and the fluidization behavior of Al_2O_3 microparticles.

Fluidization behavior of Al_2O_3 nanoparticles

Bed pressure drop and bed height: Nanoparticles notably discretely fluidized; however, they fluidize in the form of large porous agglomerates because of the notably overlap force among them (Zhou and Li, 1999, Tahmasebpoor *et al.*, 2013, Martin and Ommen, 2013). Typical fluidization curves that relate the pressure drop and the fluidizing velocity for Al_2O_3 nanoparticles are shown in Fig. 2a and b. The pressure drop increases with increasing fluidizing air velocity and random points and fluctuations in pressure drop occur in both columns (D = 4.3 cm and D = 7.1 cm). This fluctuation occurs because Al_2O_3 nanoparticles agglomerate in the case of fluidization without vibration. A smooth curve and fewer fluctuations for pressure drop with fluidizing air velocity are shown in these curves in the case of fluidization with vibration because the vibration disrupts the adhesion forces among the particles. In two cases, the pressure drop approaches a constant value with increasing fluidizing velocity.

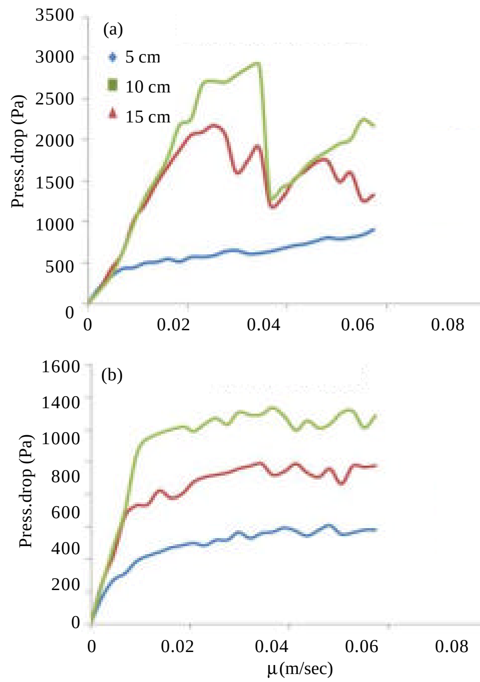

Fig. 2: Bed pressure drop as a function of the superficial gas velocity for different static bed heights for Al_2O_3 nanoparticles the column diameter is 4.3 cm: a) Without variables and B) With variables

Figure 3a and b shows the relationship between the fluidizing bed height and the fluidizing air velocity. First, the bed height curves are constant for a fixed bed with minimum fluidizing velocity. The bed height subsequently

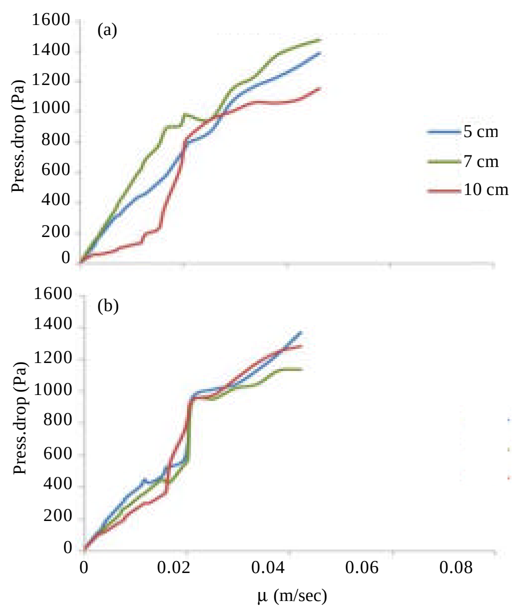

Fig. 3: Bed pressure drop as a function of the superficial gas velocity for different static bed heights for Al_2O_3 nanoparticles the column diameter is 7.1 cm: a) Without variables and B) With variables

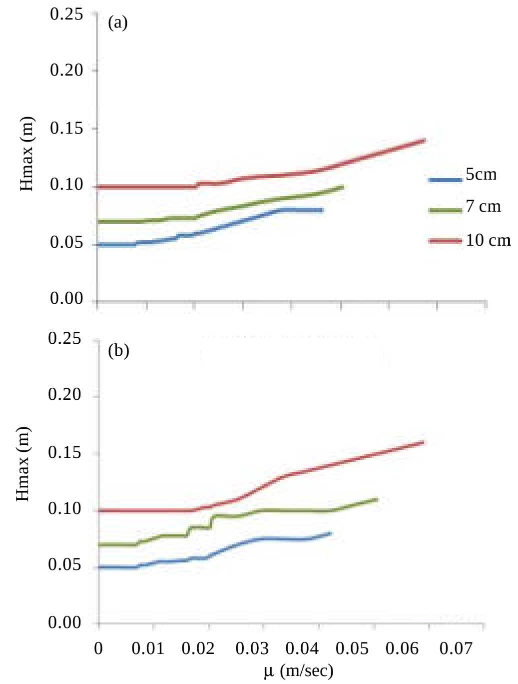

Fig. 4: Bed expansion ratio as a function of the superficial gas velocity for different static bed heights for Al_2O_3 nanoparticles; the column diameter is 4.3 cm: a) Without variables and B) With variables

increases with increasing air velocity. This situation is identical for three different static bed heights (5, 10 and 15 cm) for Al_2O_3 nanoparticles with and without vibration.

Bed expansion ratios: Bed expansion which can be easily experimentally measured is an important macroscopic characteristic of fluidized beds. The bed expansion is usually expressed in terms of the bed expansion Ratio (R). The bed expansion ratio of Al_2O_3 nanoparticles increase with increasing superficial gas velocity as shown in Fig. 4. When the gas velocity exceeds the minimum fluidization velocity, bubbles begin to form in the bed which causes bed expansion. The bed expansion ratio decreases with the application of vibration processes in the fluidized column with D = 4.3 cm as shown in Fig. 4a, b because the vibration breaks the gas bubbles in the fluidized bed. The fluidized column with D = 7.1 cm does not show any decrease in bed expansion ratio with vibration. However as shown in Fig. 4b, the expansion ratios are similar for the three static bed heights both with and without vibration (Sahoo, 2012).

Fluidization index: The FI represents the ratio of the pressure drop across the bed to the weight flux in the fluidized bed as defined by many investigators (Sahoo, 2012). The fluidization index of Al_2O_3 nanoparticles increases with increasing superficial gas velocity as shown in Fig. 5a and b. The fluidized bed with vibration shows a smooth fluidization and the FI value is approximately 1 (0.9-1.2) which indicates an almost ideal fluidization behavior, particularly in the fluidized column with D = 4.3 cm for different static bed heights (5, 10 and 15 cm) as shown in Fig. 5a. However, no effect of vibration on the FI value in the fluidized column with D = 7.1 cm is observed. Fig. 5b shows the case of a fluidized bed without vibration for different values of the FI with increasing superficial velocity.

Size of Al_2O_3 nanoparticle agglomerates: Agglomerate dimension affect the fluidization conduct of nanoparticles. The model used determined the agglomerate size for Al_2O_3 nanoparticles is based on the Richardson-Zaki and Ergun equations (Kunii and Levenspiel, 1977). The overall mass balance for the powder in the fluidized bed is given by:

$$\rho_a(1-\varepsilon_g)HA = \rho_b H_0 A = \rho_{a0}(1-\varepsilon_{g0})H_0 A \quad (1)$$

Notably, ε_g excludes the void again the agglomerates. We assume that $\rho_a \approx \rho_{a0}$ because for a nanoparticle bed, the density of agglomerates ρ_a remains approximately constant in during fluidization, the density of nanoparticles agglomerates remains constant in fluidized bed:

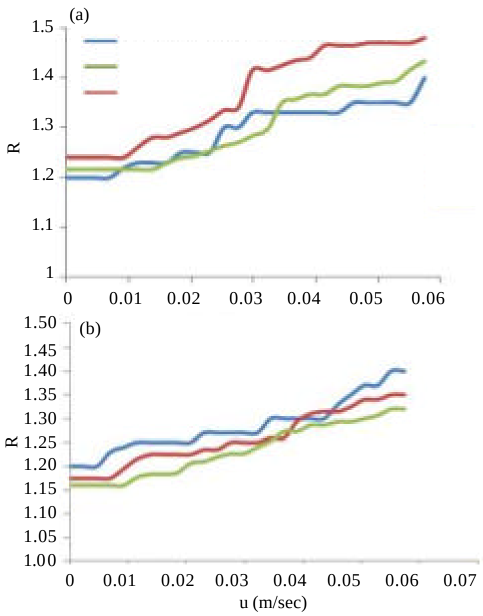

Fig. 5: Bed expansion ratio as a function of the superficial gas velocity for different static bed heights for Al_2O_3 nanoparticles; the column diameter is 4.3 cm: a) Without variables and B) With variables

$$\varepsilon_g = 1 - \frac{H_0}{H}\left(1-\varepsilon_{g0}\right) \tag{2}$$

If we imposed the R-Z equation is used (Liang *et al*., 2014), then it relates the superficial gas velocity u_g to the bed void age and terminal velocity for nano agglomerates u_t as follows:

$$u_g = u_t \varepsilon_g^n \tag{3}$$

We have shown that the Reynolds number for Al_2O_3 nanoparticle agglomerates is <1, thus, Stokes flow (creeping motion) prevails. We show that a Richardson-Zaki equation with an exponent n = 5 should be used for the Stokes flow regime according to Zhu *et al*. (2004). By combining Eq. 2 and 3, we express the relation between U_g and U_t:

$$U_t^{1/n} - U_t^{1/n}\left(1-\varepsilon_{g^o}\right)\frac{H_0}{H} = U_g^{1/n} \tag{4}$$

$$U_g^{1/n} = U_t^{1/n} - U_t^{1/n}\left(1-\varepsilon_{g0}\right)\frac{H_o}{H} \tag{5}$$

If we assume that:

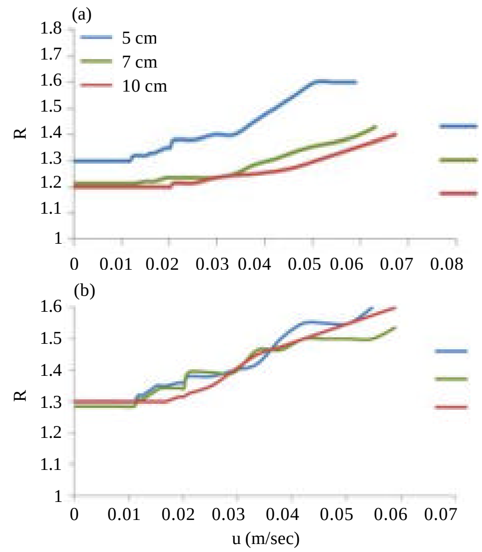

Fig. 6: Bed expension ratio as a function of the superficial gas velocity for different statics bed heights for Al_2O_3 nanoparticles; the colum diameter is 7.1 cm: a) Without variables and B) With variables

$$y = U_g^{1/n}, x = \frac{H_0}{H}, A = U_t^{1/n}\left(1-\varepsilon_{g^o}\right) B = U_t^{1/n}$$

Equation 4 and 5 can be reduced to a linear equation:

$$y = B - Ax \tag{6}$$

For Al_2O_3 nanoparticle agglomerates, Fig. 8 shows a plot of $u_g^{1/n}$ vs. H_o/H for different static bed heights with and without vibration. From a linear regression, the slope-A and y-intercept bare obtained. From, u_t and ε_{g^o} calculated from:

$$\therefore u_t = B^n \tag{7}$$

$$\varepsilon_{go} = 1 - \frac{A}{B} \tag{8}$$

The average size of nanoparticles agglomerates calculated from Stock's law as follows (Zhu *et al*., 2005):

$$d_a = \sqrt{\frac{18\,\mu u_t}{\left(\rho_a - \rho_g\right)g}} \tag{9}$$

The suppression of gas bubbles in fluidized beds of nanoparticles for gas velocities well above the minimum fluidization velocity has been related to the presence of porous light agglomerates. Thus, an important property of

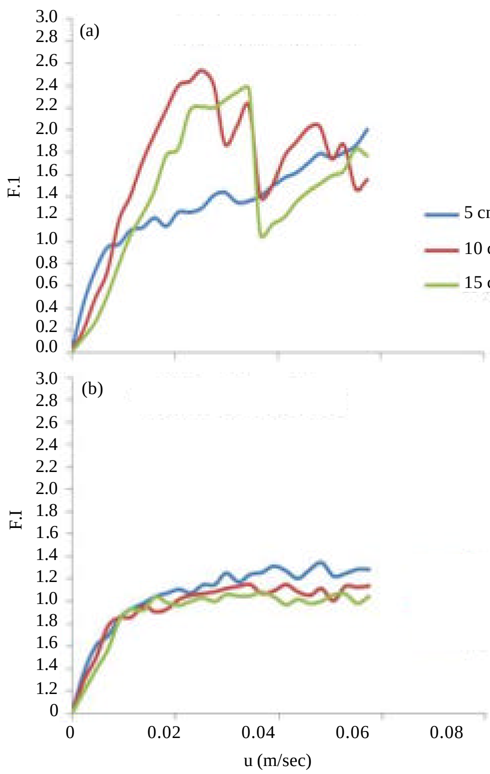

Fig. 7: Fluidization index as a function of the superficial gas velocity for different statics bed heights for Al_2O_3 nanoparticles; the colum diameter is 4.3 cm: a) Without variables and B) With variables

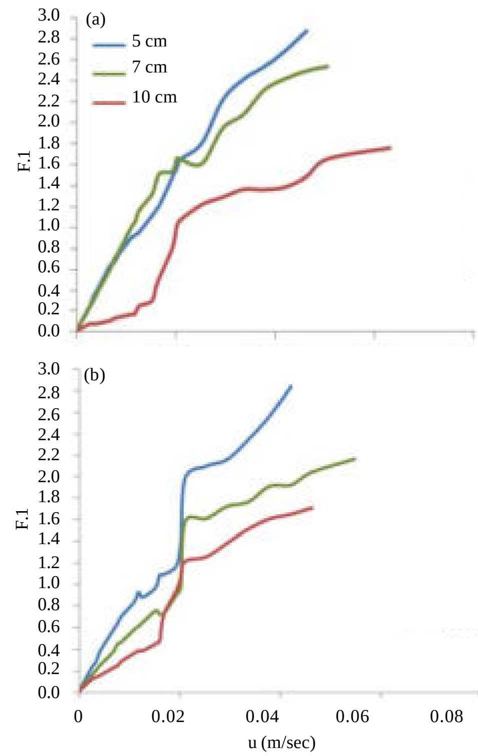

Fig. 8: Fluidization index as a function of the superficial gas velocity for different statics bed heights for Al_2O_3 nanoparticles; the colum diameter is 7.1 cm: a) Without variables and B) With variables

fluidized agglomerates is their size which is difficult to measure in an agglomerating fluidized bed. The agglomerate size with vibration decreases from 38-29% for the column with D = 4.3 and from 10-7% for the column with D = 7.1. This behavior is observed for the fluidized bed both with and without vibration but it is clearer for the fluidized bed with vibration.

Minimum fluidization velocity for Al_2O_3 nanoparticles: The minimum velocity at which a bed of particles fluidizes is a critical parameter for the design of any fluidization operation. The measured pressure drop across the bed of particles can be used to identify the minimum velocity of fluidization. As diagrammed in Fig. 7a and b, the pressure drop increases with increasing superficial air velocity until the bed expands and increases the porosity; the pressure drop then approaches a constant value when the superficial velocity increases more than the minimum fluidizing velocity. The experimental minimum fluidization velocities were measured on the basis of Fig. 7a, b; the results are listed in Table 2 and 3 for different static bed heights with and without vibration. Numerous equations have been used in the literature to

Table 2: Fluidization characteristics of Al_2O_3 nanoparticles (column diameter = 4.3 cm)

H (cm)	U_{mf} (m/sec) measured	ε_{mf}	U_{mf} (m/sec) caculated	E (%)
Without vibration				
5	0.018	0.37	0.0183	1.6
10	0.027	0.47	0.0360	25
15	0.034	0.51	0.0460	26
With vibration				
5	0.014	0.44	0.0163	14.4
10	0.022	0.53	0.0240	83
15	0.030	0.57	0.0330	9

Table 3: Fluidization characteristics of Al_2O_3 nanoparticles (column diameter = 7.1 cm)

H (cm)	U_{mf} (m/sec) measured	ε_{mf}	U_{mf} (m/sec) caculated	E (%)
Without vibration				
5	0.025	0.470	0.02509	0.39
7	0.029	0.540	0.03800	23.6
10	0.046	0.600	0.05030	8.6
With vibration				
5	0.021	0.520	0.02230	6
7	0.027	0.570	0.03200	15
10	0.035	0.630	0.03730	6.3

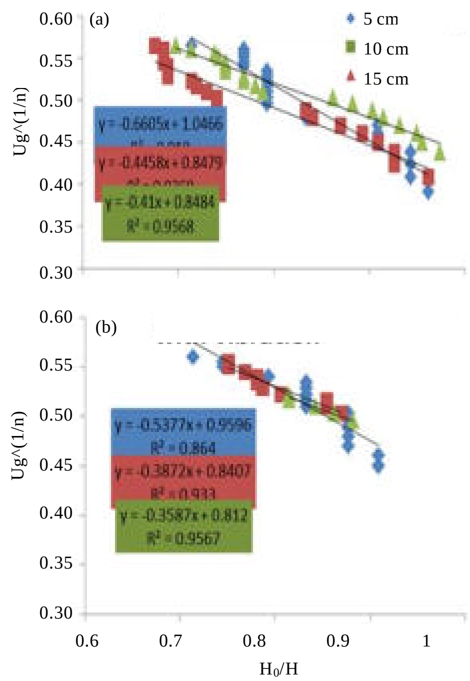

Fig. 9: A column diameter 4.3 cm

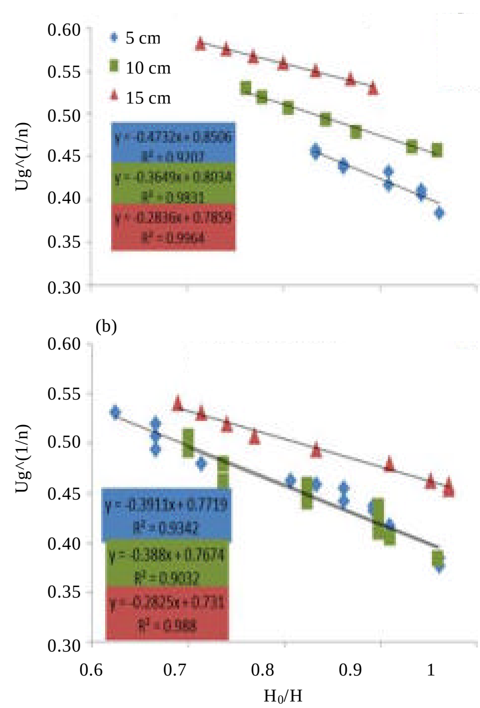

Fig. 10: A column diameter

calculate the minimum fluidizing velocity from Ergun equation we calculated Umin at Law Re. No. (Chaouki *et al*., 1985; Nam *et al*., 2004):

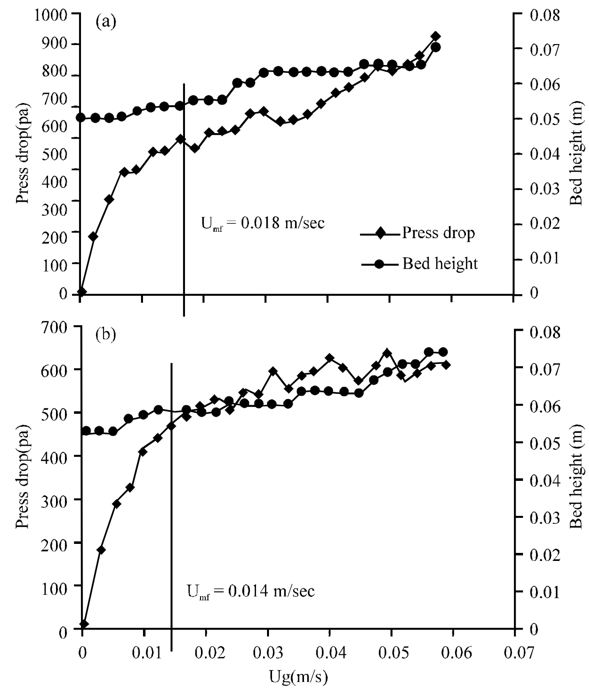

Fig. 11: Typicall fluidization curves of the pressure drop and bed height vs. Superficial gas velocity for Al_2O_3 nanoparticles; the column diameter is 4.3 cm: a) Without variables and B) With variables

$$U_{mf} = \frac{\Delta P}{H}\frac{d_a^2}{150\,\mu}\frac{\varepsilon_{gmf}}{\left(1-\varepsilon_{gmf}\right)^2} \quad (10)$$

The measured pressure drop d_a and bed height at minimum fluidization in figures were calculated using Equation 9 and 10 under the assumption that ε_{gmf} assume $\geq \varepsilon_{g^\circ}$. The minimum fluidization velocity in the fluidized column with D = 4.3 cm is less than that in the fluidized column with D = 7.1 cm because the columns have different areas and because U_{mf} increases with increasing static height bed. We observed that the minimum fluidization velocity decreases with the application of vibration processes because the vibration breaks the agglomerates and reduces the agglomerate diameter (d_a). The calculated minimum fluidization velocity is consistent with the experimental measurements. The Reynolds numbers at different static bed heights for both columns are 0.13-0.36.

Hydrodynamic fluidization behavior comparison: Our comparison is based on the presence or absence of the mechanical vibration to extinguish the effect of vibration on the static elevations in both columns. Regarding the hydrodynamic behavior of fluidizing Al_2O_3 particles, the

Table 4: Fluidization characteristics of microparticles Al_2O_3 for different fluidizg columns (Column with diameter = 4.3 cm)

H (cm)	U_{mf} (m/sec) M = measured	U_{mf} (m/sec) M = measured	E (%)	$Re_{mf} = \rho_f \alpha_\sigma U_{mf}/\mu$	$F_{mf} f = U^2_{mf}/d_\sigma g$
5	0.024	0.034	29	0.169	1.57
10	0.040	0.037	7.5	0.184	1.86
15	0.050	0.050	0	0.249	3.40

Table 5: Fluidization characteristics of microparticles Al_2O_3 for different fluidizg columns (Column with diameter = 7.1 cm)

H (cm)	U_{mf} (m/sec) M = measured	U_{mf} (m/sec) M = measured	E (%)	$Re_{mf} = \rho_f \alpha_\sigma U_{mf}/\mu$	$F_{mf} f = U^2_{mf}/d_\sigma g$
5	0.050	0.063	20.6	0.314	5.4
7	0.051	0.068	25	0.339	6.2
10	0.055	0.070	21.4	0.349	6.6

pressure drop randomly and irregularly increases with increasing gas velocity. However with the application of vibration processes, the pressure drop regularly increases; then, a simple decrease in pressure occurs at the point of minimum fluidization. Thereafter, the pressure becomes more stable. Because of strong inter particle forces, these particles of group C described by Geldart cause preferential channeling and severe gas by passing in the usual fluidized bed process. In the case with vibration, some of these forces are disrupted.

Fluidization behavior of Al_2O_3 microparticles: In this study, we conducted simple experiments on Al_2O_3 microparticles for comparison with the Al_2O_3 nanoparticles and discuss the effect of the particle size on the fluidization behavior. In the case of Al_2O_3 microparticles, the pressure drop increases and bed height increases with increasing superficial gas velocity. In addition, we calculated the minimum fluidization velocity using the Ergun equation for micro particles with a diameter = 75 μm and a Reynolds number <1. The following equation was used (Nam *et al.*, 2004):

$$U_{mf} \frac{(\phi sdp)^2}{150} \frac{\rho p\text{-}\rho g}{\mu} \left(\frac{\varepsilon_{mf^3}}{1\text{-}\varepsilon_{mf}} \right) g \quad (12)$$

where ε_{mf} is the void age at minimum fluidization which is calculated as:

$$\varepsilon_{mf} = 1\text{-}\frac{\Delta P}{H_{mf}(\rho p\text{-}\rho g)g} \quad (13)$$

Here, we did from experiments determined pressure drop and bed height at minimum fluidization obtained from the experiments. The calculated minimum fluidization velocity is consistent with the experimental results (Table 4 and 5). The minimum fluidization velocity in the fluidized column with D = 4.3 cm is less than that in the fluidized column with D = 7.1 cm because the columns have different areas and because U_{mf} increases with the increasing static height bed as shown in Table 6. The Froude numbers are 1.5-6.6 for different static heights for both columns which shows that the type of fluidization for Al_2O_3 microparticlesis aggregative fluidization. The Archimedes number was determined to be 54.33 which shows that natural convection dominates.

Table 6: Abbreviations and their units

Definition/Symbol	Units
Surface area of particles (A)	m^2
Average size of fluidized agglomerates (da)	Nm and μm
Particle size (dp)	nm and μm
Size of micron-scale agglomerate (das)	μm
Sub-agglomerates size (d)	μm
Gravity field acceleration = 9.81 (g)	m/sec^2
Bed height at minimum fluidization velocity (H_{mf})	m
Static bed height (H_o)	m
Minimum bed height (H_{min})	m
Maximum bed height (H_{max})	m
Gas velocity (u_g)	m/sec
Minimum fluidization velocity (u_{mf})	m/sec
Terminal velocity (u_t)	m/sec
Bed voidage (ε_g)	----
Porosity in each agglomerate (ε_{ag})	----
Initial bed voidage (ε_{g*})	----
Viscosity of gas (air) = 1.205×10^{-5} (μ)	Pa.s
Density of agglomerate in fluidized bed (ρ_{a*})	kg/m^3
Bulk density (ρ_b)	kg/m^3
Density of fluid (air) = 1.205 (ρ_g)	kg/m^3
Density of particles (ρ_p)	kg/m^3
ρ_b-ρ_g (ρ*)	kg/m^3
Particle sphericity (ϕ_s)	-
Pressure drop (Δ_p)	Pa = N/m^2

CONCLUSION

From the present study, the following conclusions were drawn: the minimum fluidization velocity is approximately several orders of magnitude higher than the minimum fluidization velocity of the primary nanoparticles. The minimum fluidization velocity increases with increasing static bed height because of the increase in weight bed and fluidized bed diameter.

The calculated results for the minimum fluidizing velocity for nanoparticle agglomerates are consistent with the experimental results. The agglomerate size in the gas-solid fluidized beds of nanoparticles is the most important factor that affects the fluidization quality. The fluidization quality is improved by external force techniques such as vibration. When vibration is applied to a fluidized bed, the initial bed void age increases whereas the size of the agglomerate nanoparticles decreases. The application of vibration can increase the fluidization quality of Al_2O_3particles as indicated by nearly ideal pressure-drop curves whereas the increase in equilibrium pressure drop in addition to the vibration decreases the elutriation and channeling.

The size of the agglomerate nanoparticles increases with decreasing particle size and decreases with the application vibration processes. Using vibration in the fluidized bed provides some agitation, so that, the nanoparticles do not adhere to the column wall. Thus, the vibration fragments the agglomerates.

ACKNOWLEDGEMENTS

We would like to express our deepest thanks to the staff of The Chemical Engineering Department/University of Technology for providing the facilities for this research.

REFERENCES

Chaouki, J., C. Chavarie, D. Klvana and G. Pajonk, 1985. Effect of interparticle forces on the hydrodynamic behaviour of fluidized aerogels. Powder Technol., 43: 117-125.

Kunii, D. and O. Levenspiel, 1977. Fluidization Engineering. Krieger Publishing, Malabar, Florida, ISBN:9780882755427, Pages: 534.

Liang, X., H. Duan, T. Zhou and J. Kong, 2014. Fluidization behavior of binary mixtures of nanoparticles in vibro-fluidized bed. Adv. Powder Technol., 25: 236-243.

Martin, L.D. and V.J.R. Ommen, 2013. A model to estimate the size of nanoparticle agglomerates in gas-solid fluidized beds. J. Nanopart. Res., Vol. 15, 10.1007/s11051-013-2055-x

Nam, C.H., R. Pfeffer, R.N. Dave and S. Sundaresan, 2004. Aerated vibrofluidization of silica nanoparticles. Am. Inst. Chem. Eng. J., 50: 1776-1785.

Sahoo, P., 2012. Hydrodynamic studies of course, fine and nano particles in a cylindrical fluidized spouted bed: CFD simulation. MSc Thesis, National Institute of Technology, Rourkela, India.

Tahmasebpoor, M., L. De Martin, M. Talebi, N. Mostoufi and J.R. Van Ommen, 2013. Fluidization of nanaoparticles: The effect of surface characteristics. Proceedings of the 14th International Conference on Fluidization from Fundamentals to Products, May 26-31, 2013, Hotel NH Noordwijk Conference Centre Leeuwenhorst, Noordwijkerhout, Netherlands, pp: 1-9.

Zhou, T. and H. Li, 1990. Effects of adding different size particles on fluidization of cohesive particles. Powder Technol., 102: 215-220.

Zhu, C., G. Liu, Q. Yu, R. Pfeffer and R.N. Dave *et al*., 2004. Sound assisted fluidization of nanoparticle agglomerates. Powder Technol., 141: 119-123.

Zhu, C., Q. Yu, R.N. Dave and R. Pfeffer, 2005. Gas fluidization characteristics of nanoparticle agglomerates. AIChE J., 51: 426-439.